Title

Gonadotropin-Dependent Neuregulin-1 Signaling Regulates Female Rat Ovarian Granulosa Cell Survival.

Journal

Endocrinology, 158(10)

ISSN

0888-8809

Authors

Chowdhury, Indrajit
Branch, Alicia
Mehrabi, Sharifeh
et al.

Publication Date

2017-10-01

DOI

10.1210/en.2017-00065

Peer reviewed

Gonadotropin-Dependent Neuregulin-1 Signaling Regulates Female Rat Ovarian Granulosa Cell Survival

Indrajit Chowdhury,[1,2] Alicia Branch,[1,2] Sharifeh Mehrabi,[1,2] Byron D. Ford,[4] and Winston E. Thompson[1,2,3]

[1]Department of Obstetrics and Gynecology, Morehouse School of Medicine, Atlanta, Georgia 30310; [2]Reproductive Science Research Center, Morehouse School of Medicine, Atlanta, Georgia 30310; [3]Department of Physiology, Morehouse School of Medicine, Atlanta, Georgia 30310; and [4]Division of Biomedical Sciences, University of California-Riverside School of Medicine, Riverside, California 92521

Mammalian ovarian follicular development and maturation of an oocyte competent to be fertilized and develop into an embryo depends on tightly regulated, spatiotemporally orchestrated crosstalk among cell death, survival, and differentiation signals through extra- and intraovarian signals, as well as on a permissive ovarian follicular microenvironment. Neuregulin-1 (NRG1) is a member of the epidermal growth factor–like factor family that mediates its effects by binding to a member of the erythroblastoma (ErbB) family. Our experimental results suggest gonadotropins promote differential expression of NRG1 and erbB receptors in granulosa cells (GCs), and NRG1 in theca cells during follicular development, and promote NRG1 secretions in the follicular fluid (FF) of rat ovaries. During the estrous cycle of rat, NRG1 and erbB receptors are differentially expressed in GCs and correlate positively with serum gonadotropins and steroid hormones. Moreover, *in vitro* experimental studies suggest that the protein kinase C inhibitor staurosporine (STS) causes the physical destruction of GCs by the activation of caspase-3. Exogenous NRG1 treatment of GCs delayed onset of STS-induced apoptosis and inhibited cleaved caspase-3 expressions. Moreover, exogenous NRG1 treatment of GCs alters STS-induced death by maintaining the expression of ErbB2, ErbB3, pAkt, Bcl2, and BclxL proteins. Taken together, these studies demonstrate that NRG1 is gonadotropin dependent, differentially regulated in GCs and theca cells, and secreted in ovarian FF as an intracellular survival factor that may govern follicular maturation. **(*Endocrinology* 158: 3647–3660, 2017)**

Mammalian granulosa cells (GCs) are multilayered somatic cells residing within the ovarian follicle that supports oogenesis through proliferation, differentiation, and interactive communications. These events are under the control of endocrine factors, including gonadotrophins [*i.e.*, follicle-stimulating hormone (FSH) and luteinizing hormone (LH)] (1). FSH and LH bind to their membrane receptors, which leads to a broad signaling network, including G-protein mediated activation of adenylate cyclase and subsequent production of cyclic adenosine monophosphate that, in turn, activates protein kinase A (2). During these processes, GCs produce and secrete multiple autocrine and paracrine factors, including epidermal growth factor (EGF)-like peptides (amphiregulin, epiregulin, and betacellulin) (3–8) and steroid hormones [estradiol (E2) and progesterone (P4)] that play an important role as regulators of oogenesis and folliculogenesis (9). The gonadotropin-induced production of EGF-like peptides leads to a transactivation of EGF receptor (EGFR) (10) as these peptides bind to a classical EGFR/the v-erb-b avian erythroblastic leukemia viral oncogene homolog in the erythroblastoma (ErbB) family of receptor proteins (ErbB1). Then, the ErbB receptor activates its intrinsic tyrosine kinase and downstream signaling cascades, including mitogen-activated protein kinase (MAPK)-3/1 (ERK1/2), MAPK14 (p38-a), and phosphoinositide-3-kinase/v-akt murine thymoma viral oncogene homolog (PI3K/PKB, AKT) pathways (8,

ISSN Print 0013-7227 ISSN Online 1945-7170
Printed in USA

Received 15 January 2017. Accepted 8 August 2017.
First Published Online 14 August 2017

Abbreviations: D, diestrus; E, estrus; E2, estradiol; EGF, epidermal growth factor; EGFR, epidermal growth factor receptor; ErbB, erythroblastoma; FF, follicular fluid; FSH, follicle-stimulating hormone; GC, granulosa cell; IHC, immunohistochemical; LH, luteinizing hormone; M, metestrus; MAPK, mitogen-activated protein kinase; NIH, National Institutes of Health; NRG1, neuregulin-1; P, proestrus; P4, progesterone; PMSG, pregnant mare serum gonadotropin; STS, staurosporine; WB, western blot.

11). There is accumulating evidence that also suggests EGF-like peptides act as a key regulator of follicular development in mammals (12–15).

Neuregulin-1 (NRG1) is a member of the EGF-like factor family that mediates its effects by binding to a member of ErbB family. ErbB3 and ErbB4 are two *bona fide* receptors for NRG1 (16). Upon NRG1 binding with ErbB3 or ErbB4 receptors, the bound molecules undergo heterodimerization with ErbB2, or ErbB3 heterodimerizes with ErbB4 and ErbB4 homodimerizes itself (17, 18). The receptor dimerization is followed by auto- and *trans*-phosphorylation of intracellular tyrosine residues and recruitment of an adaptor protein (PI3K/Akt and MAPK) cascade to participate in ErbB signaling to govern distinct cell-fate decisions (19). ErbB3 is a non-autonomous receptor with an impaired tyrosine kinase domain; thus, homodimers are catalytically inactive (20). The ligandless ErbB2 receptor always exists in an untethered conformation, poised to dimerize with another receptor; therefore, it acts as the preferred heterodimerization partner of all other ErbB family members (21).

NRG1 plays essential roles in the nervous system, heart, and mammary glands (22, 23). Indeed, a growing body of experimental evidence suggests that *Nrg1* is expressed in the brain of embryonic and adult mice (24–27), major endocrine glands of rhesus monkey (*Macaca mulatta*) (28), gonadotropin-dependent mice mural GCs of periovulatory follicles (29) and mouse testis (30, 31), and newt (*Cynops pyrrhogaster*) testis (32). Functional roles of NRG1 in mice suggest that NRG1 expression in GCs during ovulation enhances AREG-induced ERK1/2 phosphorylation and P4 production, and supports oocyte maturation (29, 33). Recent studies in male mice suggest LH-induced expression of NRG1 directly drives the proliferation of Leydig cells in the testis and supports the production of androgen to maintain spermatogenesis and sexual behavior of adult male mice (30). Similar studies in newts suggest that NRG1 plays a pivotal role in promoting spermatogonial proliferation by both direct effect on spermatogonia and indirect effect via somatic cells in testes (32).

Despite this evidence, there is a substantial gap in our knowledge about gonadotropin-dependent NRG1- and ErbB-receptor expression and modulation of GC survival. Therefore, in the current study, we first determined the gonadotropin-dependent expression pattern of NRG1 and ErbB receptors in undifferentiated rat GCs and ovaries, and NRG1 expression in theca cells and secretions in follicular fluid (FF). NRG1- and ErbB-receptor expressions were analyzed in GCs and ovaries during the rat estrous cycle and correlated with levels of circulating reproductive hormones. Subsequently, we determined whether the gain of NRG1 impacted the apoptosis induced by the protein kinase C inhibitor staurosporine (STS) in a rat ovarian GC model (34, 35).

Materials and Methods

Animals

Sprague–Dawley rats (female; 20 to 21 days old or 55 to 60 days old) were purchased from Charles River Laboratories (Charleston, SC). Animals were given food and water *ad libitum* and kept under a regular day/night cycle (12 hours of light, 12 hours of darkness), which was maintained automatically with lighting changes occurring at 06:00 and 18:00. All animal care procedures in this study were approved by the Institutional Animal Care and Use Committee in accordance with the guidelines of the National Institutes of Health (NIH) and the US Department of Agriculture, and approved by the Morehouse School of Medicine Animal Care and Use Committee.

Estrous cycle determination

The estrous cycles [diestrus (D), predominantly leukocytes; proestrus (P), clusters of round, well-formed nucleated epithelial cells; estrus (E), densely packed cornified squamous epithelial cells; and metestrus (M), predominantly small leukocytes with cornified squamous epithelial cells] of rats 55 to 60 days old and weighing ~230 to 250 g were tracked daily by cytological analysis of vaginal smears, using crystal violet staining at 09:00 and 12:00 (36). Only rats showing at least two consecutive 4-day cycles were used in the experiments. Rats undergoing a stage change into D, P, E, or M within this time were euthanized. This regimen precisely determined the initial onset of the estrous stage and minimized any intrastage variation. To validate the accuracy of stage determination, vaginal smears were also obtained at the time the rats were euthanized.

Hormone treatment

Immature rats (23 days old) were injected subcutaneously with 10 IU of pregnant mare serum gonadotropin (PMSG; Sigma-Aldrich) at 0, 4, 8, 24, and 48 hours with 0.10 mL of 0.9% sodium chloride to stimulate and synchronize follicular growth. Parallel control groups of rats were injected with 0.10 mL of 0.9% NaCl, and all the steps used in the PMSG-treated groups were followed.

Collection of samples

After completion of hormone (*i.e.*, PMSG) treatments of immature rats and estrous cycle determination in cycling rats, the animals were anesthetized with isoflurane inhalation and cardiac puncture was performed to collect blood samples into serum separator tubes (BD, New Jersey). The serum was separated by centrifugation (6000*g* for 20 minutes) and stored at −80°C until assayed for hormone levels. Then the ovaries were excised, being careful to avoid damage to the ovarian surface epithelium. After excision, GCs were isolated (34) from the left-side ovaries of these animals and stored at −80°C until use for immunoblot analysis. The right-side ovaries of these animals were fixed for 24 hours in 4% (weight-to-volume ratio) buffered formalin, dehydrated in 70% (volume-to-volume ratio) ethanol, embedded in paraffin, and stored at room

temperature until immunohistochemical (IHC) processing was performed.

For FF isolation, the preovulatory follicles were dissected from PMSG-treated rat ovaries at 24 and 48 hours. The FF was collected by hemisecting the isolated follicles with a scalpel blade in serum-free medium, which consisted of 15 mM HEPES, pH 7.4, Dulbecco's modified Eagle's medium/F-12 with transferrin (5 μg/mL), human insulin (2 μg/mL), hydrocortisone (40 ng/mL), and antibiotics (8 to 10 follicles per 0.2 mL). This hemisection released the FF into the medium. The solid tissue was discarded. The medium was collected and centrifuged at 1500 rpm for 10 minutes at 4°C to remove cellular debris. The supernatant containing FF was collected and stored frozen at −80°C until assayed.

GC culture and treatment with FSH

Primary GCs were isolated from sexually immature (23 to 25 days old) rat ovaries, then cultured and treated with FSH (10 and 100 ng/mL for 24 hours; National Hormone and Peptide Program oFSH; NIH) as described previously (34, 37). GCs from immature rats are referred to as undifferentiated because they lack functional LH receptors and do not produce E2 or P4 under basal conditions, and these GCs have not been exposed to pubertal cyclic gonadotrophins. However, these cells respond to FSH with respect to the production of cyclic adenosine monophosphate and induction of LH-receptor activation of the E2 and P4 biosynthetic pathways (38). Live cell phase photographs were taken via inverted microscope at ×200 magnification 24 hours after treatment.

Induction of apoptosis and treatment of recombinant NRG1

GC apoptosis was induced in serum-free medium in the presence of STS (1 μM; Sigma-Aldrich) with or without recombinant NRG1 (EGF-like domain;10 and 100 ng/mL; R&D Systems, Minneapolis, MN) for 3 hours. STS concentration and time response were used based on our previous experiments (34, 35). Live-cell phase-contrast pictures were taken to assess the survival status of GCs at 3 hours post-treatment. The percentage of apoptosis was determined by nuclear staining with Hoechst 33248 stain (12.5 ng/mL; Sigma-Aldrich) (34, 39). At least 250 to 300 cells were counted for each data point.

Western blot analysis

GC protein extracts were obtained from different treatment conditions and subjected to one-dimensional gel electrophoresis and western blot (WB) analysis (34). For one-dimensional gel electrophoresis, equal amounts of protein (25 μg) were applied to each lane. Primary antibodies were used as described in Table 1. Membranes were incubated with the appropriate secondary antibodies for 2 hours at room temperature, and antibody binding was detected by chemiluminescence (Pierce, Rockford, IL). Results of representative chemiluminescence were scanned and densitometrically analyzed using a Power Macintosh Computer (G3; Apple Computer, Cupertino, CA) equipped with a Scan Jet 6100C Scanner (Hewlett-Packard, Greeley, CO). Quantification of the scanned images was performed using NIH Image version 1.61 software (NIH, Bethesda, MD) (34).

Immunohistochemistry

Paraffin-embedded rat ovaries were serial sectioned (n = 10; 7-μm thick) from each individual ovary per rat (n = 3 rats per sample), deparaffinized in xylene washes, rehydrated, and quenched with 3% hydrogen peroxide in methanol; nonspecific sites were blocked with 20% (volume-to-volume ratio) non-immune serum/phosphate-buffered saline, and then incubated with primary anti-NRG1 antibody (1:200 dilution) for immunolocalization of NRG1. Finally, ovarian sections were incubated with secondary antibody Alexa Fluor 555-conjugated goat anti-rabbit immunoglobulin G (2 μg/mL; Molecular Probes) and subsequently incubated in 4′, 6-diamidino-2-phenylindole (1 μg/mL for 15 minutes). After thorough

Table 1. List of Antibodies Used for Western Blot Analysis and Immunohistochemistry

Peptide/ Protein Target	Name of Antibody	Name of Individual Providing the Antibody	Species Raised (Monoclonal or Polyclonal)	Research Resource Identifier (RRID)	Dilution Used
Neuregulin-1β (Nrg1)	Anti-neuregulin-1β	Santa Cruz Biotechnology	Rabbit (polyclonal)	AB_675755	1:1000[a] 1:200[b]
ErbB 1 receptor	Anti-ErbB1 receptor	Cell Signaling Technology	Rabbit (monoclonal)	AB_2230881	1:1000
ErbB 2 receptor	Anti-ErbB2 receptor	Merck Millipore	Mouse (monoclonal)	AB_1586943	1:1000
ErbB 3 receptor	Anti-ErbB3 receptor	Merck Millipore	Mouse (monoclonal)	AB_309713	1:1000
ErbB 4 receptor	Anti-ErbB4 receptor	Merck Millipore	Mouse (monoclonal)	AB_1586945	1:1000
Active caspase-3	Anti-active caspase-3	Cell Signaling Technology	Rabbit (polyclonal)	AB_2341188	1:1000
Bcl2	Anti-Bcl2	Cell Signaling Technology	Rabbit (monoclonal)	AB_2290370	1:1000
Bclxl	Anti-Bclxl	Cell Signaling Technology	Rabbit (monoclonal)	AB_2228008	1:1000
Bax	Anti-Bax	Cell Signaling Technology	Rabbit (polyclonal)	AB_10695870	1:1000
Bak	Anti-Bak	Cell Signaling Technology	Rabbit (polyclonal)	AB_2290287	1:1000
pErk1/2	Anti-pErk1/2	Cell Signaling Technology	Mouse (monoclonal)	AB_2297442	1:1000
Total Erk1/2	Anti-total Erk1/2	Cell Signaling Technology	Rabbit (monoclonal)	AB_331775	1:1000
pAkt	Anti-pAkt	Cell Signaling Technology	Rabbit (polyclonal)	AB_329825	1:1000
Total Akt	Anti-total Akt	Cell Signaling Technology	Rabbit (polyclonal)	AB_329827	1:1000
α Tubulin	Anti-α tubulin	Sigma-Aldrich	Mouse (monoclonal)	AB_477579	1:1000

[a] By western blot analysis.

[b] By immunohistochemistry.

rinsing, cover slips were mounted on slides with Vectashield mounting medium (Vector Laboratories, Burlingame, CA). Negative controls were performed omitting the primary antibody or using an isotope-matched control antibody derived from the same species. Mounted slides were examined using an Olympus BX41 microscope equipped with an Optronics Magnifier digital camera and Prior Proscan motor-driven stage (Olympus, Melville, NY). Alexa Fluor 555 has a profile similar to Texas Red stain. For each image, specific antibody staining was merged with nuclear staining (blue) using Soft Imaging System software (Olympus) that caused virtually no pixel shifting during image merging and resulted in shades of red and blue. Representative photomicrographs were arranged using Adobe PhotoShop (Adobe Systems, San Jose, CA) without any further adjustment to maintain the true nature of the findings. Fluorescence intensity of GCs and theca cells in preantral, small antral, and large antral follicles were determined using ImageJ software (NIH).

Serum hormones analysis

Serum FSH, LH, P4, and E2 concentrations were measured by the ligand assay and analysis core at the Center for Research in Reproduction, University of Virginia. The limits of detection of the assays are as follows: FSH, 0.9 to 44 ng/mL; LH, 0.07 to 74.8 ng/mL; E2, 12 to 1000 pg/mL; and P4, 0.1 to 23 ng/mL. Samples below the assay threshold were assigned the threshold value. Detailed information on the hormone analyses is available at https://med.virginia.edu/research-in-reproduction/ligand-assay-analysis-core/.

Statistical analysis

All experimental data are expressed as mean ± standard error of the mean of three independent experiments; each was replicated. Statistical analysis was carried out by one-way analysis of variance using SPSS version 11.0 (IBM, Armonk, NY). Multiple comparisons were done by Newman–Keuls test. Differences were considered significant at $P \leq 0.05$. The correlation coefficient between NRG1 and ErbB receptors, E2, and P4 were determined by linear regression analysis.

Results

Gonadotropin-dependent expression of NRG1 and ErbB receptors in GCs

To determine whether NRG1- and ErbB-receptor expression is gonadotropin dependent, immature rats were treated with PMSG for different lengths of time. Then, NRG1- and ErbB-receptor expression levels were analyzed in GCs by WB. The temporal expression pattern of NRG1 and ErbB receptors was differential in GCs in response to PMSG treatment [Fig. 1(a)]. There was significant upregulation of NRG1, ErbB1, ErbB2, and ErbB3 at 4, 8, 24, and 48 hours after PMSG treatment. In contrast to ErbB1, ErbB2, and ErbB3 receptors, ErbB4 did not change its expression at 4 and 8 hours after PMSG treatment, whereas it was significantly upregulated at 24 and 48 hours after PMSG treatment. Furthermore, correlation analysis between NRG1 and ErbB1 ($Y = 1.805 \times X + 9.302$; $R^2 = 0.5709$; $F = 17.29$; $P < 0.001$) and ErbB3 ($Y = 1.4821 \times X - 1.7342$; $R^2 = 0.7226$; $F = 33.86$; $P < 0.001$) receptors showed a significantly strong positive correlation under these experimental conditions.

In light of the dynamic changes in NRG1 expression during follicular development, IHC analysis was used to directly reveal a cell-specific pattern of NRG1 expression in the context of intact ovary from PMSG-treated rats. Interestingly, remarkable temporal and spatial differences were evident in the pattern of expression of NRG1 in ovarian tissue sections of PMSG-treated rats [Fig. 1(b) and 1(c)]. At 24 hours after PMSG treatment, NRG1 immunostaining was predominantly confined to the theca-interstitial cells and oocytes, whereas the GCs showed a low or diffuse gradient-like expression pattern within the preantral and small, and large antral follicles. At 48 hours after PMSG treatment, NRG1 immunofluorescence was strong and confined to GCs, and there was a belt-like staining of the theca-interstitial cells within the small and large antral follicles, whereas there was a strong immunostaining within the theca-interstitial cells and a diffuse gradient-like expression pattern within GCs in the preantral follicles. Interestingly, at 48 hours after PMSG treatment, the oocyte was clearly devoid of NRG1 in preantral and small and large antral follicles. Also, NRG1 immunostaining was found in the cytoplasm of GCs and theca-interstitial cells within the follicles. These IHC analyses revealed that NRG1 protein was heterogeneously expressed during gonadotropin-stimulated follicular maturation.

Gonadotropin-dependent secretions of NRG1 in FF

FF is the secretory product of GCs, theca cells, and blood plasma that provides an important microenvironment for the development of oocytes. Therefore, we analyzed gonadotropin-dependent secretion of NRG1 in the FF. PMSG treatment in immature rats had time-dependent, significant stimulatory effects on NRG1 secretions in the FF [Fig. 2(a)]. In addition, concentrations of NRG1 in the FF were positively correlated with the serum levels of E2 ($Y = 0.706 \times X - 8.5231$; $R^2 = 0.811$; $F = 30.03$; $P < 0.001$) and P4 ($Y = 0.078 \times X - 1.1139$; $R^2 = 0.7396$; $F = 19.88$; $P < 0.0029$) at 24 and 48 hours after PMSG treatment. These results support a strong stimulatory effect of PMSG on secretions of NRG1 in FF.

FSH-dependent expression of NRG1 in GCs

To determine the direct effects of gonadotropin on NRG1 expression in GCs, we examined the dose-dependent effects of FSH on NRG1 expression in GCs. As shown in phase-contrast photomicrographs [Fig. 2(b)], GCs have a fibroblastic appearance *in vitro* in serum-free medium (control GCs), and were altered in

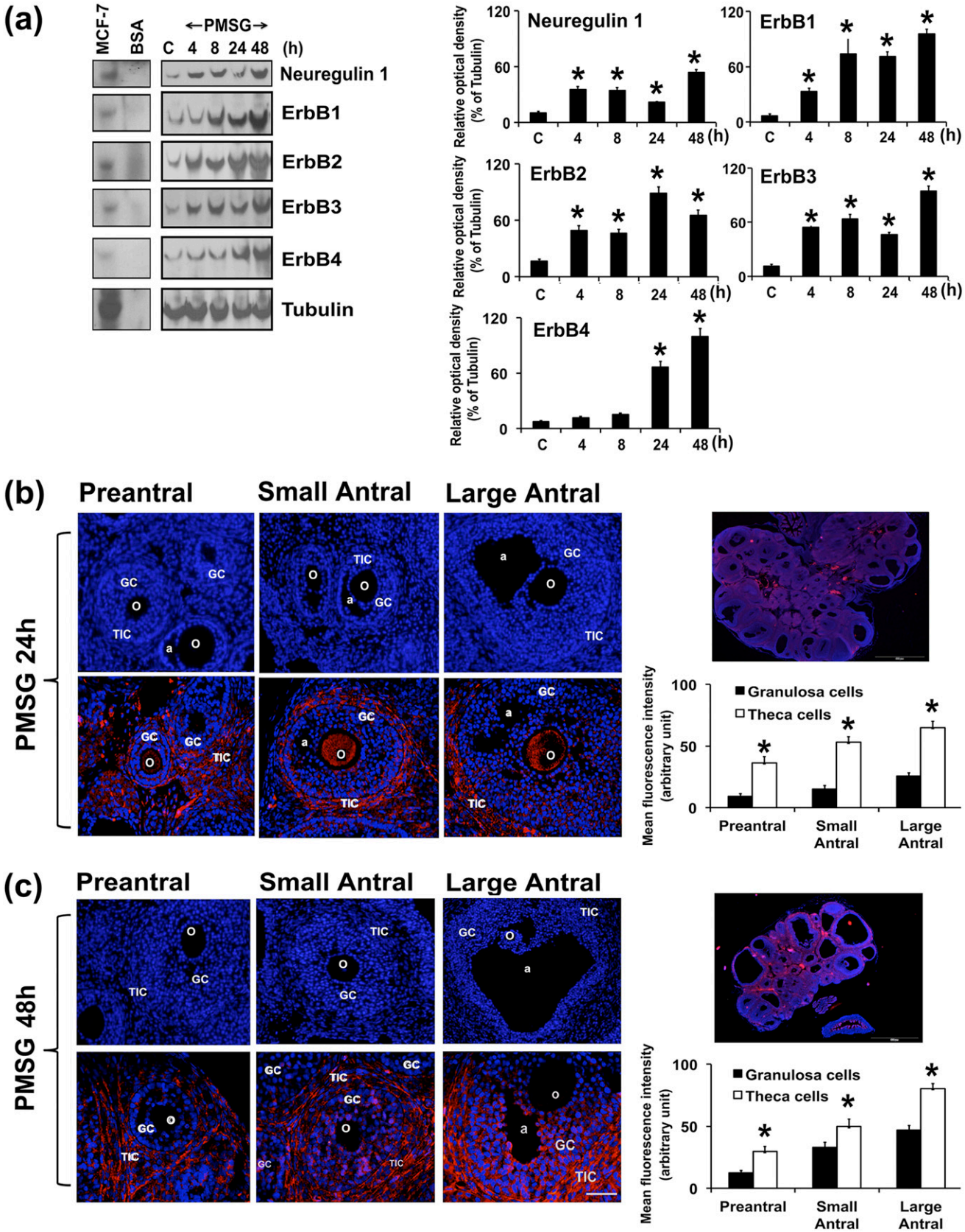

Figure 1. Gonadotropin-dependent expression of NRG1 and the ErbB family of receptors in GCs. Immature rats (23 days old) were treated with or without PMSG for different lengths of time. (a) Representative WB analysis of protein levels of NRG1 and ErbB receptors in GCs isolated from two ovaries per rat per sample. Equal amounts of protein were applied to each lane. α-Tubulin was used as an internal control. Bar diagrams represent the densitometric analyses of protein in WBs. MCF-7 cell line protein extract was used as a positive control; BSA was used as negative control. $^*P \leq 0.05$ relative to control group. (b, c) Immunocolocalization of endogenous NRG1 with Alexa Fluor 594-labeled (red) secondary

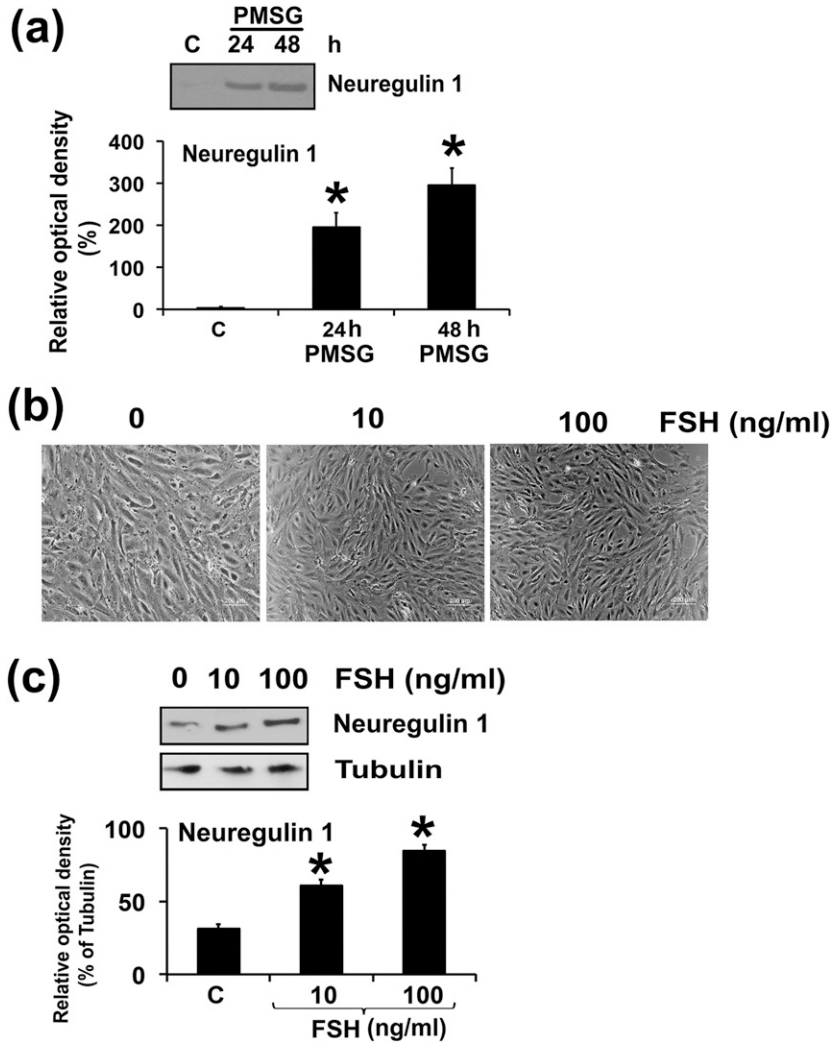

Figure 2. (a) Gonadotropin-dependent secretions of NRG1 in FF. Immature rats (23 days old) were treated with or without PMSG for 24 and 48 hours (n = 3 rats per time point). FF was collected from two ovaries per rat per sample and analyzed for NRG1 protein concentrations by WB. (b, c) Gonadotropin-dependent expressions of NRG1 in rat GCs. Undifferentiated GCs were isolated from two ovaries per rat per sample and grown in culture dishes. Thereafter, GCs were treated either with or without FSH (10 and 100 ng/mL) for 24 hours. Parallel control GCs were maintained without any treatments. (b) Representative phase photomicrographs of live cells were taken under an inverted microscope at ×200 magnification at 24 hours after treatment in the absence or presence of FSH. (c) Representative WB analysis of protein levels of NRG1 in GCs cultured from two ovaries per rat per sample, and treated with or without FSH for 24 hours. Equal amounts of protein were applied to each lane. α-Tubulin was used as an internal control. Bar diagram represents the densitometric analyses of NRG1 in WB of three independent experiments. Data given as mean ± standard error of the mean. *$P \leq 0.05$ with control group. C, parallel control.

morphology in the presence of FSH. Interestingly, FSH significantly increased NRG1 expression in GCs dose dependently [Fig 2(c)]. Correlation analysis further demonstrated a strong positive correlation (Y = 1.7323 × X − 65.127; R^2 = 0.7412; F = 20.05; $P < 0.0029$) between FSH doses and NRG1 protein concentrations in GCs.

Differential expression pattern of NRG1 and ErbB receptors during the estrous cycle

The pubertal activation of the female reproductive endocrine axis is the start of cyclical events that directly influence the function and anatomy of the pituitary, ovary, uterus, external genitalia, and the mammary glands. Therefore, we investigated NRG1- and ErbB-receptor expressions in GCs during the estrous cycle of rat and correlated the expression with concentrations of serum gonadotropins and steroid hormones.

As shown in Fig. 3(a), the serum FSH concentration was significantly highest in the P stage and lowest in the M and D stages. Serum LH concentration was higher in P, E, and M stages. As expected, a profound surge in serum E2 occurred during the P stage and lowest concentration was measured in the M stage [Fig. 3(b)], whereas P4 concentration was highest during M stage. There was no significant difference in P4 concentrations during the D, P, and E stages.

Next, we examined the expression pattern of NRG1 and ErbB receptors throughout the estrous cycle in GCs. NRG1 and ErbB receptors were differentially expressed throughout the estrous cycle [Fig. 3(c) and 3(d)]. There was significant upregulation of NRG1 during the P and M stages, whereas ErbB1- and ErbB4-receptor concentrations were significantly higher in the E and M stages. Interestingly, ErbB3-receptor concentration was significantly higher during the P, E, and M stages, and higher than ErbB1-, ErbB2-, and ErbB4-receptor concentrations. Moreover, compared with the ErbB3 receptor, the NRG1 showed a strong positive

Figure 1. (Continued). antibody in gonadotropin-treated rat ovary at (b) 24 and (c) 48 hours (n = 3 rats per time point). Representative photomicrographs of whole ovary at 24 and 48 hours are depicted separately. The nucleus was counterstained with 4′,6-diamidino-2-phenylindole (blue). Bar diagrams represent the mean fluorescence intensity of Alexa Fluor 594 in GCs and theca cells in preantral, small antral, and large antral follicles at (b) 24 and (c) 48 hours. *$P \leq 0.05$ relative to NRG1 expression between GCs and theca cells in preantral and small and large antral follicles. All the data and numerical values (presented as mean ± standard error of the mean) are represented from three independent experiments performed for each individual group. a, antrum; BSA, bovine serum albumin; o, oocyte; TIC, theca-interstitial cell.

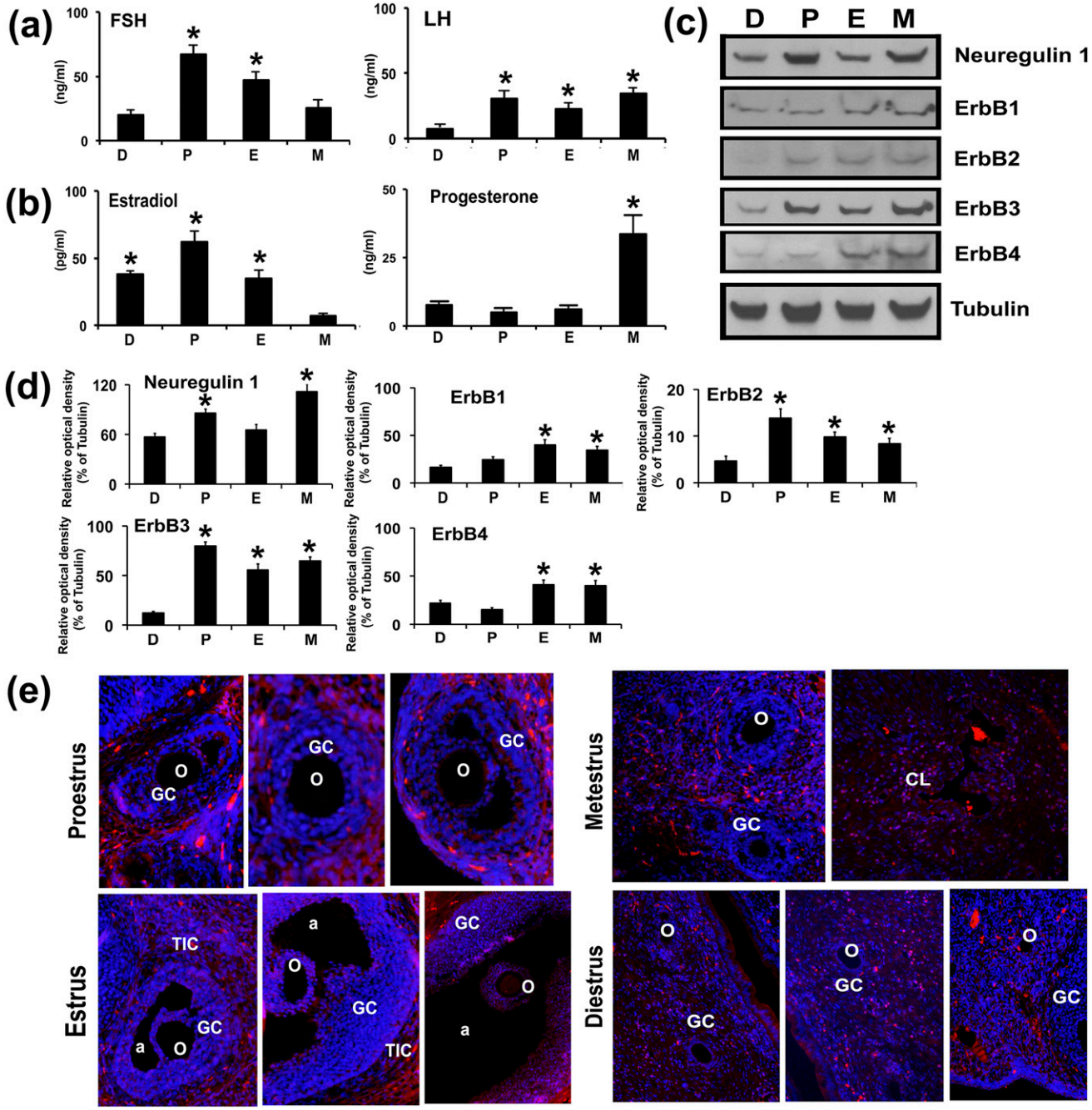

Figure 3. Expression of NRG1 and ErbB receptors in GCs during the rat estrous cycle. Blood serum and GCs were collected throughout the estrous cycle. Bar diagrams represent the mean values of serum (a) FSH and LH and (b) E2 and P4 of the D, P, E, and M stages during the estrous cycle. (c) Representative WB analysis of protein levels of NRG1 and ErbB receptors in GCs isolated from two ovaries per rat per stage of estrous cycle. Equal amounts of protein were applied to each lane. α-Tubulin was used as an internal control. (d) Bar diagrams represent the densitometric analyses of NRG1 and ErbB receptors in WB. (e) Immunocolocalization of endogenous NRG1 with Alexa Fluor 594 labeled (red) secondary antibody in rat ovary during different stages of the estrous cycle. The nucleus was counterstained with 4′,6-diamidino-2-phenylindole (blue). All numerical values are represented as mean ± standard error of the mean of three independent experiments. A total three rats per stage of estrous cycle were used. $^*P \leq 0.05$ among the group. a, antrum; o, oocyte; TIC, theca-interstitial cell.

correlation during the rat estrous cycle. Interestingly, ErbB2 concentration was lower than that of ErbB1, ErbB3, and ErbB4 receptors but was significantly higher in the P, E, and M stages of estrous cycle.

Furthermore, IHC staining of NRG1 in rat ovarian sections during the estrous cycle demonstrated significant differences in temporal and spatial expression patterns of NRG1. As shown in Fig. 3(e), NRG1 immunostaining had a belt-like signaling appearance in the theca-interstitial cells at P and E stages, whereas the GCs showed a differential, gradient-like expression pattern within the preantral and small and large antral follicles.

Interestingly, oocytes showed more intense fluorescent signals in antral follicles in the E stage. In the M stage, the corpus luteum showed intense NRG1 immunostaining. However, the D stage showed a weak diffuse pattern of NRG1 immunostaining in GCs of primary follicles and lacked the strong, belt-like NRG1 immunostaining in the theca-interstitial cells.

Exogenous NRG1 treatment inhibited activation of cleaved caspase-3 in GCs

FSH-dependent growth and differentiation of GCs support follicle maturation. In this process, many of the signaling pathways orchestrate ovarian follicle development through GC survival. To elucidate the role of NRG1 in GC survival, immature rat GCs were grown to 95% to 100% confluence, and treated with STS (1 μM) for 3 hours in exogenous recombinant NRG1-pretreated (for 24 hours) or -cotreated GCs in serum-free medium (34, 35). STS has been extensively used *in vitro* at higher (micromolar) concentrations as an initiator of apoptosis in many different cell types, whereas at lower (nanomolar) concentrations, STS acts as an inhibitor of protein kinase C (34, 35, 40, 41). GCs treated with STS showed significantly high numbers of cells with apoptotic morphology exhibiting cell detachment; loss of cell processes; membrane shrinkage, as evidenced by curling of cells; and formation of apoptotic bodies when compared with the control group [Fig. 4(a)]. At 3 hours after STS exposure, 50% ± 3% of GCs displayed apoptotic morphology compared with parallel control cells (2% ± 0.3%; $P < 0.05$). Both doses of NRG1-pretreated (24 hours) GCs, and the lower-dose (10 ng/mL) NRG1-cotreated GCs with STS treatment showed significantly higher numbers of cells with apoptotic nuclear morphology when compared with the control (*i.e.*, untreated) group [Fig. 4(a)]. Interestingly, the higher dose (100 ng/mL) of NRG1-cotreated GCs with STS treatment showed significantly fewer cells with apoptotic nuclear morphology when

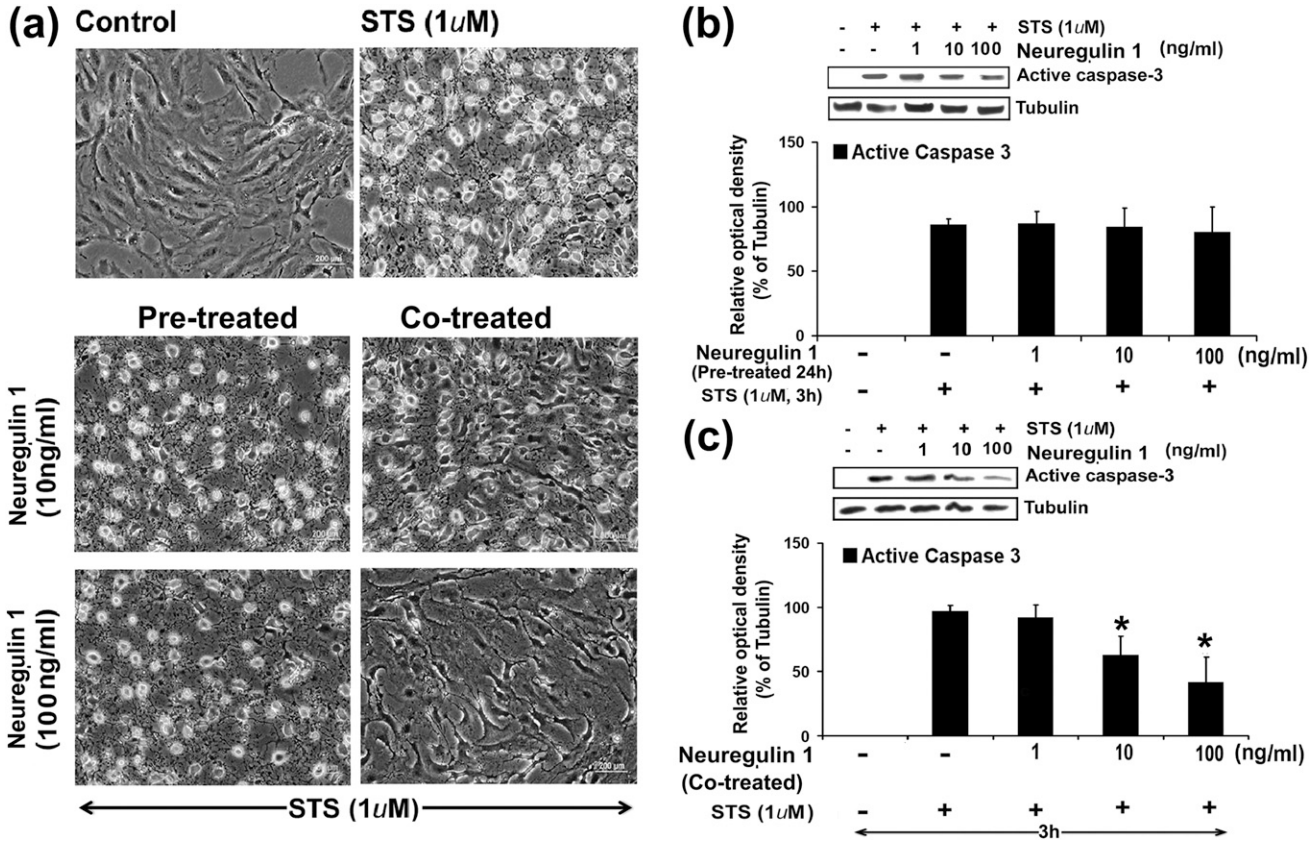

Figure 4. Effects of exogenous treatment of NRG1 on PKC inhibitor STS-induced apoptosis in undifferentiated rat GCs. Undifferentiated GCs were isolated from two ovaries per rat per sample and grown in culture dishes. Thereafter, GCs were pretreated with NRG 1 for 24 hours, then treated with STS (1 μM) for 3 hours in serum-free medium, or GCs were cotreated with NRG 1 along with STS (1 μM) for 3 hours in serum-free medium. (a) STS induced morphological changes in presence or absence of NRG1 in GCs. Representative phase photomicrographs of live cells were taken under an inverted microscope at ×200 magnification at 3 hours after treatment with STS in NRG1-pretreated or cotreated groups. (b, c) Representative WB analysis of STS-induced active caspase-3 expressions in (b) NRG1-pretreated or (c) NRG1-cotreated GCs for 3 hours. Equal amounts of protein were applied to each lane and WB analyzed for active caspase-3 expressions. α-Tubulin was used as an internal control. Bar diagrams represent the densitometric analyses of protein in WB from three independent experiments that were performed for each individual group. Data given as mean ± standard error of the mean. $^*P \leq 0.05$.

compared with STS alone or with NRG1-pretreated (24 hours) and lower-dose (10 ng/mL) NRG1-cotreated groups.

Caspase-3 is a potent effector caspase that targets several specific cellular proteins, causing a number of changes associated with cell death. Therefore, the effect of the exogenous recombinant NRG1 treatment on active caspase-3 expression was evaluated by WB in the STS-treated (3 hours) GCs with or without NRG1 in the pretreated (for 24 hours) or cotreated condition. At the higher dose (100 ng/mL), NRG1-cotreated GCs with STS treatment showed significantly lower expression of active caspase-3 when compared with STS alone or with the NRG1-pretreated (10 and 100 ng/mL for 24 hours) and lower-dose (10 ng/mL) NRG1-cotreated groups [Fig. 4(b) and 4(c)]. These results were corroborated by GC morphological analysis in the presence or absence of NRG1 with STS treatment [Fig. 4(a)]. Based on these results, we selected the 100 ng/mL NRG1 cotreatment dose with STS treatment of 3 hours for all other experimental studies.

Based on the results shown in Fig. 4, undifferentiated GCs were cotreated with NRG1 in the presence or absence of STS, and the percentage of apoptosis was determined by nuclear staining with Hoechst 33248 stain. The exogenous cotreatment of NRG1 provided marked inhibition against STS-induced apoptosis [Fig. 5(a)], in agreement with the morphological differences observed under these experimental conditions.

To explore the mechanism by which NRG1 prevents apoptosis in undifferentiated GCs treated with STS, we examined the relative expression levels of pro- and antiapoptotic proteins in the Bcl family. There were significantly enhanced levels of Bax and Bak, and decreased levels of Bcl2 and Bclxl protein expression in STS-treated GCs [Fig. 5(b)]. Interestingly, when GCs were cotreated with NRG1 in the presence of STS, there was significantly less inhibition of Bcl2 and Bclxl levels, and less increase of Bax and Bak levels compared with that of the STS-treated parallel group. These results were corroborated by the quantitative expression analysis as represented by Bax-to-Bcl2, Bax-to-Bclxl, Bak-to-Bcl2, and Bak-to-Bclxl ratios and active caspase-3 expression [Fig. 5(c)]. The Bax-to-Bcl2, Bax-to-Bclxl, Bak-to-Bcl2, and Bak-to-Bclxl ratios were significantly two- to threefold lower in STS-treated GCs in presence of NRG1.

It has been demonstrated that NRG1, via ErbB receptors, activates downstream effectors, including Akt and Erk (19). Therefore, we explored whether STS-treated GCs in the presence of NRG1 affect phosphorylation of Akt and Erk. Treatment of GCs with NRG1 stimulated the phosphorylation of Akt but not Erk [Fig. 5(d)]. STS treatment significantly inhibited phosphorylation of Akt and Erk in GCs [Fig. 5(d)], whereas Akt phosphorylation was maintained in GCs treated with STS in the presence of NRG1. However, treatment with NRG1 did not maintain the phosphorylation of Erk in the presence of STS [Fig. 5(d)].

ErbB3 and ErbB4 are two *bona fide* receptors for NRG1. Therefore, we analyzed ErbB2-, ErbB3-, and ErbB4-receptor expression patterns under these experimental conditions. STS treatment significantly inhibited ErbB2, ErbB3, and ErbB4 expression in GCs [Fig. 5(e)]. Treatment of GCs with NRG1 alone stimulated the levels of ErbB2, ErbB3, and ErbB4 compared with those of the controls. Importantly, treatment of GCs with STS in the presence of NRG1 prevented the STS-induced inhibition of ErbB2 and ErbB3 expression.

Discussion

Gonadotropins regulate folliculogenesis in the ovary as a recurring set of events that culminates in the ability to produce steroid hormones and fertile ova. To achieve success in these events, GCs, along with theca cells, act harmoniously to elicit an orchestrated temporal expression pattern of steroidogenic enzymes, which determines the ovarian production of androgens P4 and E2 (9, 37, 42–44) through multiple molecular coordination including EGF family members (4, 5, 7, 29, 33, 45). Following this rationale, our attempt to reveal the nature of the ovarian functional cycle focused on characterization of NRG1- and ErbB-receptor expression patterns during the process of follicular development.

In light of the earlier observation that gonadotropin-dependent secretion of E2 and P4 with ovarian follicular maturation (46, 47), we evaluated serum steroid levels along with the expression patterns of the NRG1 and ErbB receptors, which are implicated in the regulation of folliculogenesis (29, 33). Our results demonstrate a rapid and dynamic change in NRG1- and ErbB-receptor expression in GCs during follicular development. The biphasic patterns of NRG1 expression in response to PMSG were corroborated by ErbB3-receptor expression in GCs. Interestingly, the immediate response of GCs to gonadotropins on NRG1-, ErbB1-, ErbB2-, and ErbB3-receptor expression, but not ErbB4-receptor expression, was readily observed at 4 and 8 hours. Moreover, IHC localization of NRG1 of gonadotropin-primed ovaries suggests that NRG1 expression in GCs, interstitial cells, and theca cells may be involved in proliferation, differentiation, and maturation of follicles (29, 33). In this respect, NRG1 expression in GCs and ovarian follicles probably resembles a similar scenario characterizing the constitutively active testicular spermatogonial and Sertoli cells, in which NRG1 is upregulated in response to FSH (31). Also the *in vitro* results of our study showed

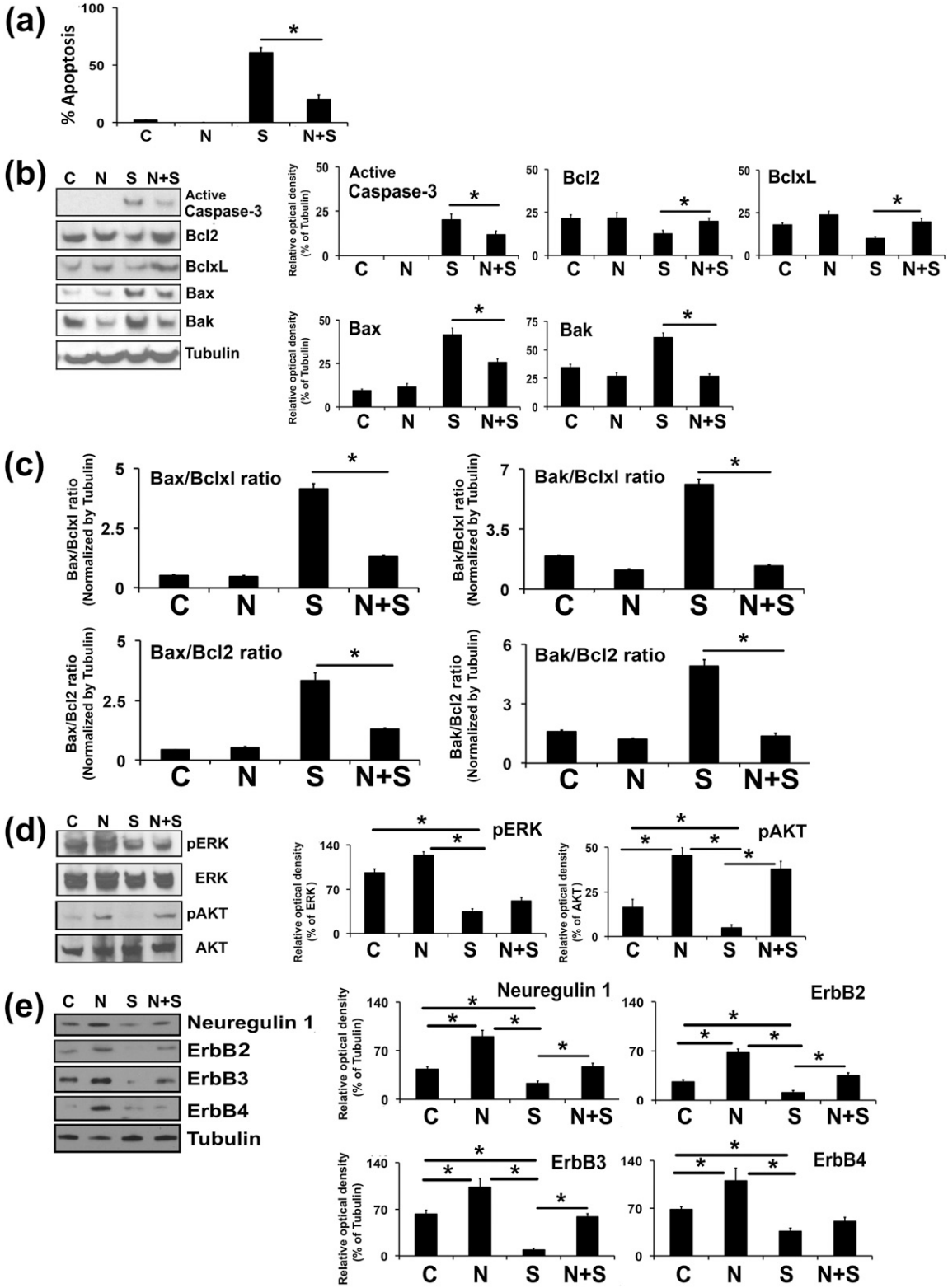

Figure 5. Effects of exogenous cotreatment of NRG1 on the PKC inhibitor STS-induced apoptosis in undifferentiated rat GCs. Undifferentiated GCs were isolated from two ovaries per rat per sample and grown in culture dishes. Thereafter, GCs were cotreated with NRG1 along with STS (1 μM) for 3 hours in serum-free medium. (a) Bar graph represents the percentage of GCs displaying nuclear morphologic changes characteristic of apoptosis. (b) Representative WB analysis of protein levels in GCs treated by STS in the presence and absence of NRG1 for cleaved caspase-3, Bcl2, Bclxl, Bax, and Bak. α-Tubulin was used as an internal control. Bars represent the densitometric analyses of protein in WBs. (c) Bars represent the mean ± standard error of the mean of Bax-to-Bclxl, Bax-to-Bcl2, Bak-to-Bclxl, and Bak-to-Bcl2 ratios of protein levels normalized to α-tubulin from three independent experiments. (d) Representative WB analysis of protein levels in GCs treated by STS in the presence and absence of NRG1 for total Erk1/2, phospho-Erk1/2 (pErk1/2), and total Akt and phospho-Akt. Bars represent the densitometric analyses of protein in WBs. (e) Representative WB analysis of protein levels in GCs treated by STS in the presence and absence of NRG1 for NRG1 and ErbB

FSH-dependent expression of NRG1 in GCs. These results further indicate that the gonadotropin-dependent local production of NRG1 plays an important role in regulating the function of GCs similar to that of other EGF family members (4, 5, 7). Of note, the *NRG1* gene encodes multiple isoforms, which are produced through alternative splicing and promoter use (48); however, these variants differ in their *N*-terminal sequence and all the variants share a conserved EGF-like domain that is responsible for receptor activation (48, 49). It has been demonstrated that the final phase of follicular growth and maturation is driven by FSH through a sharp increase in EGFR expression in GCs (50). FSH also is known to induce expression of LH receptors in the GCs (38), permitting them to release EGFR ligands in response to preovulatory LH. By coordinating receptor expression and ligand release, FSH endows fully grown follicles with the capacity to activate EGFR signaling at ovulation (50). Thus, our results suggest that PMSG promotes follicular development through EGF-ligand NRG1 and ErbB receptors that may support remodeling of the late follicular environment for an efficient and coordinated response to ovulatory signals (50).

Interestingly, during the estrous cycle, NRG1 expression in preantral, antral, or preovulatory follicles is also increased with ovarian development; this was corroborated by serum gonadotropin levels and is in agreement with other EGF factors (4, 5, 7, 45). Our study also provided evidence that NRG1 is expressed and localized within the GCs of follicles, oocytes, and corpus luteum during the rat estrus cycle. These results indicate increases in NRG1 protein expression are correlated with events associated with follicular development. Moreover, our results strongly suggest that gonadotropin-dependent expression of ErbB3 may be a possible binding partner of NRG1 to heterodimerize with the ErbB2 receptor during follicular maturation.

Our study findings suggest that the exogenous treatment of NRG1 abrogated STS-induced activation of caspase 3 by preventing the expression of two major proapoptotic factors, Bax and Bak, most likely acting through ErbB3 by downstream activation of the pAkt/pErk-Bcl2/Bclxl pathway in undifferentiated GCs (51–53). As a result, NRG1 preserved the viability of GCs by tilting the balance in favor of survival. The apoptosis-inhibiting effects of Bcl2 and Bclxl are counteracted by the proapoptotic proteins Bax and Bak. Any imbalance of the Bax and Bak versus Bcl2 and Bclxl ratios tilts the scales toward cell death and sensitized cells to a wide variety of cell-death stimuli, including all chemotherapeutic drugs, radiation, hypoxia, or growth factor withdrawal, and enhances the resistance of cells to the cytotoxic effects (35, 54–59). Interestingly, ectopic Bcl2 overexpression in sensitive cell lines prevented the triggering of apoptotic stimuli, thereby supporting the role of the Bax/Bcl-2 rheostat as a key checkpoint (55, 60). The broad resistance to cell death, occurring upon the intracellular balance of the Bax-to-Bcl2, Bax-to-Bclxl, Bak-to-Bcl2, and Bak-to-Bclxl ratios, has potential relevance for cell behavior, including cell invasion, adhesion, or metastatic potential (54).

Our results demonstrate that treatment with NRG1 stimulated the phosphorylation of Akt, which was not inhibited by cotreatment with STS. Akt is involved in induction of the antiapoptotic Bcl2 factors as an adaptive response to cellular stress (61). Moreover, our results indicated that NRG1 treatment maintained ErbB2 and ErbB3 expression in the GCs, corresponding to the increased survival of GCs, and may be related to downstream signaling events mediated by ErbB2 and ErbB3 compared with the STS-treated GCs. Downstream signaling for ErbB3 primarily involves PI3K/Akt, and ErbB3 is required for survival, proliferation, and differentiation of other cells, potentially through PI3K signaling (6, 29, 35, 62–64). Currently, there are data available to support the physiological functions for NRG1-induced ErbB2 and ErbB3 signaling (65, 66) during the development of the sympathetic nervous system in mice (67) and the upper spinous layers of the skin (68); in preservation of differentiation of human trophoblasts and inhibition of apoptosis (65, 66); and balance between luminal and basal breast epithelium (69). The homozygous deletions of ErbB2, ErbB3, and NRG1 result in embryonic lethality, a phenotype often accompanied by placental defects (26, 70, 71). The loss of ErbB3 decreased PI3K/Akt signaling and impaired mammary epithelial cells along with luminal lineage (69), and promoted attenuation of tumorigenesis via a tumor-specific increase in caspase-3–mediated apoptosis (72). In human trophoblasts, receptor knockdown and neutralization experiments revealed that both ErbB2 and ErbB3 are involved in NRG1-mediated activation of Akt1 (65, 66). In the current study, we show that NRG1 treatment supports GC survival. Whether the PI3K/Akt signaling pathway is mechanistically linked to ErbB2 and ErbB3 expression and GC survival requires further investigation.

Figure 5. (Continued). receptors. α-Tubulin was used as an internal control. Bar diagrams represent the densitometric analyses of protein in WBs. Equal amounts of protein were applied to each lane and the WB was analyzed for different proteins. Data, given as mean ± standard error of the mean, are representative of three independent experiments that were performed for each individual group. $^*P \leq 0.05$ between STS and NRG1 plus STS groups. C, control; S, staurosporine; N, Neuregulin-1.

In conclusion, our results suggest that gonadotropins promote expression of NRG1 in GCs and theca cells, ErbB receptors in GCs, and secretion of NRG1 in the FF. Interestingly, exogenous NRG1 stimulated the phosphorylation of AKT and the expression of ErbB receptors. The ability of NRG1 to reduce STS-induced GC death was associated with the maintenance of ErbB2 and ErbB3 expression and cell survival signaling proteins. This study suggests that NRG1 serves as a survival factor that may govern follicular maturation.

Acknowledgments

We thank Sidney A. Pitts, Molecular Histology Laboratory, Morehouse School of Medicine, for immunohistochemistry. Part of this work was presented at the American Society for Cell Biology Annual Meeting, New Orleans, Louisiana, December 14–18, 2013; 14th Research Centers in Minority Institutions' "Transdisciplinary Collaborations: Evolving Dimensions of US and Global Health Equity," Washington, District of Columbia, December 1–3, 2014; 49th Annual Meeting of the Society for the Study of Reproduction, San Diego, California, July 16–20, 2016; and Morehouse School of Medicine/Tuskegee University/University of Alabama, Birmingham, Comprehensive Cancer Center Partnership 2016, Atlanta, Georgia, July 26–27, 2016.

Financial Support: This study was supported in part by National Institutes of Health Grants 1SC3GM113751, 1RO1HD057235, G12RR03034, and P50HD28934. This investigation was conducted in a facility constructed with support from Research Facilities Improvement Grant C06RR018386 from National Institutes of Health National Center for Research Resources.

Correspondence and Reprint Requests: Indrajit Chowdhury, PhD, Department Of Obstetrics and Gynecology, Reproductive Science Research Center, Morehouse School of Medicine, 720 Westview Drive Southwest, Atlanta, Georgia 30310. E-mail: indrajitfbs@gmail.com or ichowdhury@msm.edu.

Disclosure Summary: The authors have nothing to disclose.

References

1. Havelock JC, Rainey WE, Carr BR. Ovarian granulosa cell lines. *Mol Cell Endocrinol*. 2004;**228**(1-2):67–78.
2. Prochazka R, Blaha M, Nemcova L. Signaling pathways regulating FSH- and amphiregulin-induced meiotic resumption and cumulus cell expansion in the pig. *Reproduction*. 2012;**144**(5):535–546.
3. Ashkenazi H, Cao X, Motola S, Popliker M, Conti M, Tsafriri A. Epidermal growth factor family members: endogenous mediators of the ovulatory response. *Endocrinology*. 2005;**146**(1):77–84.
4. Ben-Ami I, Armon L, Freimann S, Strassburger D, Ron-El R, Amsterdam A. EGF-like growth factors as LH mediators in the human corpus luteum. *Hum Reprod*. 2009;**24**(1):176–184.
5. Berasain C, Avila MA. Amphiregulin. *Semin Cell Dev Biol*. 2014;**28**:31–41.
6. Park Y, Maizels ET, Feiger ZJ, Alam H, Peters CA, Woodruff TK, Unterman TG, Lee EJ, Jameson JL, Hunzicker-Dunn M. Induction of cyclin D2 in rat granulosa cells requires FSH-dependent relief from FOXO1 repression coupled with positive signals from Smad. *J Biol Chem*. 2005;**280**(10):9135–9148.
7. Riese II DJ, Cullum RL. Epiregulin: roles in normal physiology and cancer. *Semin Cell Dev Biol*. 2014;**28**:49–56.
8. Shimada M, Hernandez-Gonzalez I, Gonzalez-Robayna I, Richards JS. Paracrine and autocrine regulation of epidermal growth factor-like factors in cumulus oocyte complexes and granulosa cells: key roles for prostaglandin synthase 2 and progesterone receptor. *Mol Endocrinol*. 2006;**20**(6):1352–1365.
9. Chowdhury I, Thomas K, Thompson WE. Prohibitin (PHB) roles in granulosa cell physiology. *Cell Tissue Res*. 2016;**363**(1):19–29.
10. Conti M, Hsieh M, Park JY, Su YQ. Role of the epidermal growth factor network in ovarian follicles. *Mol Endocrinol*. 2006;**20**(4):715–723.
11. Hsieh M, Thao K, Conti M. Genetic dissection of epidermal growth factor receptor signaling during luteinizing hormone-induced oocyte maturation. *PLoS One*. 2011;**6**(6):e21574.
12. Adhikari D, Liu K. Molecular mechanisms underlying the activation of mammalian primordial follicles. *Endocr Rev*. 2009;**30**(5):438–464.
13. Fang L, Yu Y, Zhang R, He J, Sun YP. Amphiregulin mediates hCG-induced StAR expression and progesterone production in human granulosa cells. *Sci Rep*. 2016;**6**:24917–24928.
14. Silva JR, van den Hurk R, de Matos MH, dos Santos RR, Pessoa C, de Moraes MO, de Figueiredo JR. Influences of FSH and EGF on primordial follicles during in vitro culture of caprine ovarian cortical tissue. *Theriogenology*. 2004;**61**(9):1691–1704.
15. Tamura M, Sasano H, Suzuki T, Fukaya T, Funayama Y, Takayama K, Takaya R, Yajima A. Expression of epidermal growth factors and epidermal growth factor receptor in normal cycling human ovaries. *Hum Reprod*. 1995;**10**(7):1891–1896.
16. Mei L, Xiong WC. Neuregulin 1 in neural development, synaptic plasticity and schizophrenia. *Nat Rev Neurosci*. 2008;**9**(6):437–452.
17. Graus-Porta D, Beerli RR, Daly JM, Hynes NE. ErbB-2, the preferred heterodimerization partner of all ErbB receptors, is a mediator of lateral signaling. *EMBO J*. 1997;**16**(7):1647–1655.
18. Tzahar E, Waterman H, Chen X, Levkowitz G, Karunagaran D, Lavi S, Ratzkin BJ, Yarden Y. A hierarchical network of interreceptor interactions determines signal transduction by Neu differentiation factor/neuregulin and epidermal growth factor. *Mol Cell Biol*. 1996;**16**(10):5276–5287.
19. Citri A, Yarden Y. EGF-ERBB signalling: towards the systems level. *Nat Rev Mol Cell Biol*. 2006;**7**(7):505–516.
20. Carraway III KL, Sliwkowski MX, Akita R, Platko JV, Guy PM, Nuijens A, Diamonti AJ, Vandlen RL, Cantley LC, Cerione RA. The erbB3 gene product is a receptor for heregulin. *J Biol Chem*. 1994;**269**(19):14303–14306.
21. Garrett TP, McKern NM, Lou M, Elleman TC, Adams TE, Lovrecz GO, Kofler M, Jorissen RN, Nice EC, Burgess AW, Ward CW. The crystal structure of a truncated ErbB2 ectodomain reveals an active conformation, poised to interact with other ErbB receptors. *Mol Cell*. 2003;**11**(2):495–505.
22. Falls DL. Neuregulins: functions, forms, and signaling strategies. *Exp Cell Res*. 2003;**284**(1):14–30.
23. Parodi EM, Kuhn B. Signalling between microvascular endothelium and cardiomyocytes through neuregulin. *Cardiovasc Res*. 2014;**102**(2):194–204.
24. Birchmeier C. ErbB receptors and the development of the nervous system. *Exp Cell Res*. 2009;**315**(4):611–618.
25. Li Y, Lein PJ, Ford GD, Liu C, Stovall KC, White TE, Bruun DA, Tewolde T, Gates AS, Distel TJ, Surles-Zeigler MC, Ford BD. Neuregulin-1 inhibits neuroinflammatory responses in a rat model of organophosphate-nerve agent-induced delayed neuronal injury. *J Neuroinflammation*. 2015;**12**:64.
26. Meyer D, Birchmeier C. Distinct isoforms of neuregulin are expressed in mesenchymal and neuronal cells during mouse development. *Proc Natl Acad Sci USA*. 1994;**91**(3):1064–1068.

27. Simmons LJ, Surles-Zeigler MC, Li Y, Ford GD, Newman GD, Ford BD. Regulation of inflammatory responses by neuregulin-1 in brain ischemia and microglial cells in vitro involves the NF-kappa B pathway. *J Neuroinflammation*. 2016;**13**(1):237.
28. Zhao WJ. Expression and localization of Neuregulin-1 (Nrg1) and ErbB2/ErbB4 receptors in main endocrine organs of the rhesus monkey. *Int J Endocrinol Metab*. 2013;**11**(3):162–166.
29. Noma N, Kawashima I, Fan HY, Fujita Y, Kawai T, Tomoda Y, Mihara T, Richards JS, Shimada M. LH-induced neuregulin 1 (NRG1) type III transcripts control granulosa cell differentiation and oocyte maturation. *Mol Endocrinol*. 2011;**25**(1):104–116.
30. Umehara T, Kawashima I, Kawai T, Hoshino Y, Morohashi KI, Shima Y, Zeng W, Richards JS, Shimada M. Neuregulin 1 regulates proliferation of Leydig cells to support spermatogenesis and sexual behavior in adult mice. *Endocrinology*. 2016;**157**(12):4899–4913.
31. Zhang J, Eto K, Honmyou A, Nakao K, Kiyonari H, Abé S. Neuregulins are essential for spermatogonial proliferation and meiotic initiation in neonatal mouse testis. *Development*. 2011; **138**(15):3159–3168.
32. Oral O, Uchida I, Eto K, Nakayama Y, Nishimura O, Hirao Y, Ueda J, Tarui H, Agata K, Abé S. Promotion of spermatogonial proliferation by neuregulin 1 in newt (*Cynops pyrrhogaster*) testis. *Mech Dev*. 2008;**125**(9-10):906–917.
33. Kawashima I, Umehara T, Noma N, Kawai T, Shitanaka M, Richards JS, Shimada M. Targeted disruption of Nrg1 in granulosa cells alters the temporal progression of oocyte maturation. *Mol Endocrinol*. 2014;**28**(5):706–721.
34. Chowdhury I, Xu W, Stiles JK, Zeleznik A, Yao X, Matthews R, Thomas K, Thompson WE. Apoptosis of rat granulosa cells after staurosporine and serum withdrawal is suppressed by adenovirus-directed overexpression of prohibitin. *Endocrinology*. 2007; **148**(1):206–217.
35. Chowdhury I, Thompson WE, Welch C, Thomas K, Matthews R. Prohibitin (PHB) inhibits apoptosis in rat granulosa cells (GCs) through the extracellular signal-regulated kinase 1/2 (ERK1/2) and the Bcl family of proteins. *Apoptosis*. 2013;**18**(12):1513–1525.
36. Inderdeo DS, Edwards DR, Han VK, Khokha R. Temporal and spatial expression of tissue inhibitors of metalloproteinases during the natural ovulatory cycle of the mouse. *Biol Reprod*. 1996;**55**(3): 498–508.
37. Chowdhury I, Thomas K, Zeleznik A, Thompson WE. Prohibitin regulates the FSH signaling pathway in rat granulosa cell differentiation. *J Mol Endocrinol*. 2016;**56**(4):325–336.
38. Bebia Z, Somers JP, Liu G, Ihrig L, Shenker A, Zeleznik AJ. Adenovirus-directed expression of functional luteinizing hormone (LH) receptors in undifferentiated rat granulosa cells: evidence for differential signaling through follicle-stimulating hormone and LH receptors. *Endocrinology*. 2001;**142**(6):2252–2259.
39. Chowdhury I, Branch A, Olatinwo M, Thomas K, Matthews R, Thompson WE. Prohibitin (PHB) acts as a potent survival factor against ceramide induced apoptosis in rat granulosa cells. *Life Sci*. 2011;**89**(9-10):295–303.
40. Tee AR, Proud CG. Staurosporine inhibits phosphorylation of translational regulators linked to mTOR. *Cell Death Differ*. 2001; **8**(8):841–849.
41. Antonsson A, Persson JL. Induction of apoptosis by staurosporine involves the inhibition of expression of the major cell cycle proteins at the G(2)/m checkpoint accompanied by alterations in Erk and Akt kinase activities. *Anticancer Res*. 2009;**29**(8):2893–2898.
42. Hickey GJ, Chen SA, Besman MJ, Shively JE, Hall PF, Gaddy-Kurten D, Richards JS. Hormonal regulation, tissue distribution, and content of aromatase cytochrome P450 messenger ribonucleic acid and enzyme in rat ovarian follicles and corpora lutea: relationship to estradiol biosynthesis. *Endocrinology*. 1988;**122**(4): 1426–1436.
43. Miller WL, Auchus RJ. The molecular biology, biochemistry, and physiology of human steroidogenesis and its disorders. *Endocr Rev*. 2011;**32**(1):81–151.
44. Miller WL, Bose HS. Early steps in steroidogenesis: intracellular cholesterol trafficking. *J Lipid Res*. 2011;**52**(12):2111–2135.
45. Garnett K, Wang J, Roy SK. Spatiotemporal expression of epidermal growth factor receptor messenger RNA and protein in the hamster ovary: follicle stage-specific differential modulation by follicle-stimulating hormone, luteinizing hormone, estradiol, and progesterone. *Biol Reprod*. 2002;**67**(5):1593–1604.
46. Hirshfield AN. Development of follicles in the mammalian ovary. *Int Rev Cytol*. 1991;**124**:43–101.
47. Hsueh AJ, McGee EA, Hayashi M, Hsu SY. Hormonal regulation of early follicle development in the rat ovary. *Mol Cell Endocrinol*. 2000;**163**(1-2):95–100.
48. Mei L, Nave KA. Neuregulin-ERBB signaling in the nervous system and neuropsychiatric diseases. *Neuron*. 2014;**83**(1):27–49.
49. Jones JT, Ballinger MD, Pisacane PI, Lofgren JA, Fitzpatrick VD, Fairbrother WJ, Wells JA, Sliwkowski MX. Binding interaction of the heregulinbeta egf domain with ErbB3 and ErbB4 receptors assessed by alanine scanning mutagenesis. *J Biol Chem*. 1998; **273**(19):11667–11674.
50. El-Hayek S, Demeestere I, Clarke HJ. Follicle-stimulating hormone regulates expression and activity of epidermal growth factor receptor in the murine ovarian follicle. *Proc Natl Acad Sci USA*. 2014; **111**(47):16778–16783.
51. Andersson H, Rehm S, Stanislaus D, Wood CE. Scientific and regulatory policy committee (SRPC) paper: assessment of circulating hormones in nonclinical toxicity studies III. female reproductive hormones. *Toxicol Pathol*. 2013;**41**(6):921–934.
52. Hu CL, Cowan RG, Harman RM, Quirk SM. Cell cycle progression and activation of Akt kinase are required for insulin-like growth factor I-mediated suppression of apoptosis in granulosa cells. *Mol Endocrinol*. 2004;**18**(2):326–338.
53. Chun SY, Billig H, Tilly JL, Furuta I, Tsafriri A, Hsueh AJ. Gonadotropin suppression of apoptosis in cultured preovulatory follicles: mediatory role of endogenous insulin-like growth factor I. *Endocrinology*. 1994;**135**(5):1845–1853.
54. Tilly JL, Billig H, Kowalski KI, Hsueh AJ. Epidermal growth factor and basic fibroblast growth factor suppress the spontaneous onset of apoptosis in cultured rat ovarian granulosa cells and follicles by a tyrosine kinase-dependent mechanism. *Mol Endocrinol*. 1992; **6**(11):1942–1950.
55. Slot KA, Voorendt M, de Boer-Brouwer M, van Vugt HH, Teerds KJ. Estrous cycle dependent changes in expression and distribution of Fas, Fas ligand, Bcl-2, Bax, and pro- and active caspase-3 in the rat ovary. *J Endocrinol*. 2006;**188**(2):179–192.
56. Dharap SS, Chandna P, Wang Y, Khandare JJ, Qiu B, Stein S, Minko T. Molecular targeting of BCL2 and BCLXL proteins by synthetic BCL2 homology 3 domain peptide enhances the efficacy of chemotherapy. *J Pharmacol Exp Ther*. 2006;**316**(3):992–998.
57. Filali M, Frydman N, Belot MP, Hesters L, Gaudin F, Tachdjian G, Emilie D, Frydman R, Machelon V. Oocyte in-vitro maturation: BCL2 mRNA content in cumulus cells reflects oocyte competency. *Reprod Biomed Online*. 2009;**19**(Suppl 4):4309.
58. Jozwicki W, Brożyna AA, Walentowicz M, Grabiec M. Bilateral aggressive malignant granulosa cell tumour with essentially different immunophenotypes in primary and metastatic lesions comprising predominantly sarcomatoid and fibrothecomatous patterns - looking for prognostic markers: a case report. *Arch Med Sci*. 2011;**7**(5):918–922.
59. Matsuda F, Inoue N, Manabe N, Ohkura S. Follicular growth and atresia in mammalian ovaries: regulation by survival and death of granulosa cells. *J Reprod Dev*. 2012;**58**(1):44–50.
60. Parborell F, Abramovich D, Tesone M. Intrabursal administration of the antiangiopoietin 1 antibody produces a delay in rat follicular development associated with an increase in ovarian apoptosis mediated by changes in the expression of BCL2 related genes. *Biol Reprod*. 2008;**78**(3):506–513.
61. Gibson EM, Henson ES, Villanueva J, Gibson SB. MEK kinase 1 induces mitochondrial permeability transition leading to apoptosis

independent of cytochrome c release. *J Biol Chem*. 2002;**277**(12): 10573–10580.
62. Fulda S, Gorman AM, Hori O, Samali A. Cellular stress responses: cell survival and cell death. *Int J Cell Biol*. 2010;**2010**:214074.
63. Alam H, Weck J, Maizels E, Park Y, Lee EJ, Ashcroft M, Hunzicker-Dunn M. Role of the phosphatidylinositol-3-kinase and extracellular regulated kinase pathways in the induction of hypoxia-inducible factor (HIF)-1 activity and the HIF-1 target vascular endothelial growth factor in ovarian granulosa cells in response to follicle-stimulating hormone. *Endocrinology*. 2009; **150**(2):915–928.
64. Gonzalez-Robayna IJ, Falender AE, Ochsner S, Firestone GL, Richards JS. Follicle-stimulating hormone (FSH) stimulates phosphorylation and activation of protein kinase B (PKB/Akt) and serum and glucocorticoid-lnduced kinase (Sgk): evidence for A kinase-independent signaling by FSH in granulosa cells. *Mol Endocrinol*. 2000;**14**(8):1283–1300.
65. Fan HY, Liu Z, Shimada M, Sterneck E, Johnson PF, Hedrick SM, Richards JS. MAPK3/1 (ERK1/2) in ovarian granulosa cells are essential for female fertility. *Science*. 2009;**324**(5929): 938–941.
66. Fock V, Plessl K, Draxler P, Otti GR, Fiala C, Knöfler M, Pollheimer J. Neuregulin-1-mediated ErbB2-ErbB3 signalling protects human trophoblasts against apoptosis to preserve differentiation. *J Cell Sci*. 2015;**128**(23):4306–4316.
67. Fock V, Plessl K, Fuchs R, Dekan S, Milla SK, Haider S, Fiala C, Knöfler M, Pollheimer J. Trophoblast subtype-specific EGFR/ERBB4 expression correlates with cell cycle progression and hyperplasia in complete hydatidiform moles. *Hum Reprod*. 2015; **30**(4):789–799.
68. Britsch S, Li L, Kirchhoff S, Theuring F, Brinkmann V, Birchmeier C, Riethmacher D. The ErbB2 and ErbB3 receptors and their ligand, neuregulin-1, are essential for development of the sympathetic nervous system. *Genes Dev*. 1998;**12**(12):1825–1836.
69. Piepkorn M, Predd H, Underwood R, Cook P. Proliferation-differentiation relationships in the expression of heparin-binding epidermal growth factor-related factors and erbB receptors by normal and psoriatic human keratinocytes. *Arch Dermatol Res*. 2003;**295**(3):93–101.
70. Balko JM, Miller TW, Morrison MM, Hutchinson K, Young C, Rinehart C, Sánchez V, Jee D, Polyak K, Prat A, Perou CM, Arteaga CL, Cook RS. The receptor tyrosine kinase ErbB3 maintains the balance between luminal and basal breast epithelium. *Proc Natl Acad Sci USA*. 2012;**109**(1):221–226.
71. Natale DR, Starovic M, Cross JC. Phenotypic analysis of the mouse placenta. *Methods Mol Med*. 2006;**121**:275–293.
72. Riethmacher D, Sonnenberg-Riethmacher E, Brinkmann V, Yamaai T, Lewin GR, Birchmeier C. Severe neuropathies in mice with targeted mutations in the ErbB3 receptor. *Nature*. 1997; **389**(6652):725–730.